

Metals and Ceramics Division

**Effect of Surface Condition and Heat Treatment on Corrosion of
Type 316L Stainless Steel in a Mercury Thermal Convection Loop**

S. J. Pawel
J. R. DiStefano
E. T. Manneschildt

Date Published: July 2000

Prepared for the
U. S. Department of Energy
Spallation Neutron Source

Prepared by the
OAK RIDGE NATIONAL LABORATORY
Oak Ridge, Tennessee 37831-6285
operated by
UT-Battelle, LLC
for the
U.S. DEPARTMENT OF ENERGY
under contract DE-AC05-00OR22725

CONTENTS

	Page
FIGURES	v
TABES	vii
ABSTRACT	ix
1. INTRODUCTION	1
2. EXPERIMENTAL	3
2.1 LOOP FABRICATION	3
2.2 FILLING WITH MERCURY	6
2.3 LOOP OPERATION	7
3. RESULTS AND DISCUSSION	9
3.1 INTRODUCTION	9
3.2 NOMINAL 316L SPECIMENS	9
3.3 SPECIMENS COATED WITH GOLD	11
3.4 OXIDIZED SPECIMENS	15
3.5 POLISHED SPECIMENS	16
3.6 SIMULATED RADIATION DAMAGE SPECIMENS	16
3.7 SENSITIZED SPECIMENS	18
3.8 ETCHED SPECIMENS	21
3.9 WELDED SPECIMENS	22
3.10 316LN SPECIMENS	22
3.11 TENSILE SPECIMENS	25
3.12 LOOP PRETREATMENT	26
4.0 CONCLUSIONS	29
ACKNOWLEDGMENTS	31
REFERENCES	33

FIGURES

Figure	Page
1. Schematic of the thermal convection loop design. The distance between thermocouple wells on each vertical section is about 70 cm in the actual loop, and the vertical sections are separated by about 45 cm	3
2. Dimensions (in cm) of rectangular coupons and miniature tensile specimens	5
3. Post-test cross section of Coupon 5H2 in the as-polished condition. This coupon was exposed near the top of the hot leg in Loop 5 at a temperature of about 304°C. The surface which was wetted by the Hg has become porous. Most areas of the coupon surface reveal less surface porosity than shown in this photomicrograph	10
4. Representative backscattered electron image and microprobe results from labeled areas from Coupon 5H2 (annealed 316L). Note that the peak associated with Ni is essentially absent from the surface scan (Region 1) and the peaks associated with Cr are significantly reduced	11
5. Post-test appearance of Specimen 6C18, which was gold coated on one side (top photo) and was protected from gold coating on the opposite side by a circular support stand (bottom photo). The side formerly coated with gold retains no gold coloration but residual Hg clings to large portions of the surface with a low contact angle. The majority of the opposite side, protected from gold coating, is essentially unaffected by exposure to Hg	13
6. As-polished cross section of Specimen 6C18 on the side formerly coated with gold. Note the surface roughness and irregular penetration	14
7. Post-test appearance of Specimen 6H4, which was polished on one side (top photo) and in the surface ground condition on the opposite side (bottom photo). Note significant clinging Hg on the polished side (film of Hg with low contact angle) but little Hg and only minor discoloration on the unpolished side	17
8. As-polished cross section of Coupon 5H4, which was polished on the side shown. Note that the surface is generally smooth and only limited penetration is indicated	18
9. Post-test appearance of Specimen 6C21, which was implanted with Fe to simulate irradiation damage on one side (top photo, circular region) and was protected from implantation on the other side (bottom photo). No Hg beads were observed to cling to this specimen	19
10. As-polished cross section of Coupon 6C6, which was implanted with Fe to simulate irradiation damage on the side shown. The extent of penetration is both irregular and very shallow	20

11. Post-test appearance of Specimen 6C23, which was sensitized (20 h at 650°C) prior to the test. A dark film adheres to most of this specimen (but not to adjacent specimens in the chain). Tiny beads of Hg can be observed clinging to the specimen, particularly near the holes in the coupon	21
12. Post-test appearance of Coupons 6H12 (top) and 5H12 (bottom) indicating the range of Hg wetting associated with the weld pad on each coupon. The apparent “darkness” of the weld pad in the center of each coupon is an artifact of the relatively rough surface as opposed to actual discoloration. Coupon 6H12 has quite of lot of clinging Hg where Coupon 5H12 (exposed at the same temperature) has almost none	23
13. Post-test appearance of Coupon 6C30, which is type 316LN stainless steel. The irregular dark pattern on the surface was common to these specimens, but little Hg was observed clinging to the surface at any location	24
14. As-polished cross section of Coupon 6C14 (type 316LN stainless steel). Much of the coupon surface has attack/penetration similar to that shown here (about 5 μm deep)	24
15. As-polished cross section of a miniature tensile specimen (5C5) showing only limited penetration/attack at the specimen surface	25

TABLES

Table	Page
1. Composition of alloy 316L SS TCL tubing and specimens. Data from mill certification for each material, given in weight percent	4
2. Nominal temperatures at each “corner” of the thermal convection loops described here along with equivalent data for TCL 1 (a previous 316L TCL). Approximately a $\pm 2/C$ drift over the duration of the experiment was measured at each location	8
3. Weight change data for 316L specimens coated with gold on one side	12

ABSTRACT

Two thermal convection loops (TCLs) fabricated from 316L stainless steel and containing mercury and a variety of 316L coupons representing variable surface conditions and heat treatments have been operated continuously for 2000 h. Surface conditions included surface ground, polished, gold-coated, chemically etched, bombarded with Fe to simulate radiation damage, and oxidized. Heat treatments included solution treated, welded, and sensitized. In addition, a nitrogen doped 316L material, termed 316LN, was also examined in the solution treated condition. Duplicate TCLs were operated in this experiment – both were operated with a 305°C peak temperature, a 65°C temperature gradient, and mercury velocity of 1.2 m/min – but only one included a 36 h soak in Hg at 310°C just prior to operation to encourage wetting. Results indicate that the soak in Hg at 310°C had no lasting effect on wetting or compatibility with Hg. Further, based on examination of post-test wetting and coupon weight loss, only the gold-coated surfaces revealed significant interaction with Hg. In areas wetted significantly by Hg, the extreme surface of the stainless steel (ca 10 μm) was depleted in Ni and Cr compared to the bulk composition.

1. INTRODUCTION

The Spallation Neutron Source (SNS) will generate neutrons via interaction of a 1.0 GeV proton beam with a liquid mercury target. Type 316L/316LN austenitic stainless steel (SS) has been selected as the primary target containment material¹ based on a favorable combination of several factors, including resistance to corrosion by Hg, well characterized behavior in a radiation environment, and the absence of a significant ductile-brittle transition temperature such as that found in ferritic stainless steels.

The energy deposited in the target by the proton beam (design basis is presently 2 MW) will be removed by circulating the mercury through standard heat exchangers. Various fluid dynamics computations and simulations of conditions expected in the target predict maximum bulk mercury temperatures on the order of 150°C with nominal temperatures closer to 100-120°C. The mercury temperature at the target inlet is expected to be near ambient temperature.

As a result of the temperature gradient in flowing Hg, one of the potential compatibility problems under investigation in support of the SNS Project is thermal gradient mass transfer. In this form of corrosion, dissolution of the container material by the liquid in relatively high temperature (high solubility) regions is accompanied by deposition of solute in relatively colder regions.² As a result, corrosion of the high temperature region is not limited by system equilibrium and is potentially accelerated over what would be experienced in an isothermal/stagnant system. In addition, in the cold regions, deposition of solute material has been known to cause flow disruptions and can even plug flow paths in liquid metal loops.³ Among the major alloying elements of stainless steels, nickel is expected to have the highest solubility in mercury⁴ at SNS operating temperatures, and therefore this element may be the most susceptible to mass transfer.

At the expected SNS operating temperatures, pure mercury does not readily wet 316/316L stainless steel. Without chemical wetting (characterized macroscopically by a low contact angle), any potential corrosion process is inhibited. However, mercury can be made to wet 316/316L in air or vacuum by raising the temperature to 225-275/C.⁵ Despite the relatively low expected operating temperatures, chemical wetting of containment surfaces may be encouraged in the SNS target by a combination of several factors:

1. the presence of thermal hot spots,
2. radiation damage in the presence of Hg, and

3. generation of fresh (oxide-free) surfaces that result from potential cavitation and thermal shock/fatigue loading to which the target containment material will be exposed.

To examine potential “worst case” corrosion, it is desirable to develop wetting in the tests for material compatibility with mercury. Previous compatibility experiments for the SNS target station^{6,7} utilized thermal convection loops (TCLs) with relatively high peak temperatures (near 300°C) and, in some cases, a small amount of gallium added to the circulating mercury in order to encourage wetting.

The results for the 316L exposures⁶ indicated that the Ga addition did not contribute to enhanced wetting but that coupon wetting and weight loss seemed to be a strong function of temperature. Specifically, coupons exposed to Hg above 250°C exhibited the development of a porous surface layer substantially depleted of Ni and Cr, while coupons exposed at lower temperatures revealed no interaction with the Hg (no change in weight, appearance, or microstructure).

In the original 316L TCLs, all of the coupons in the exposure were fabricated from mill-annealed material with a standard surface ground finish. To examine other material conditions, the original TCL experiment was “duplicated” by operating with the same TCL conditions while including coupons representing a number of different surface and microstructure conditions. In addition, a TCL with an identical coupon array was operated by soaking the entire loop filled with Hg at 310°C for 36 hours (to try to develop wetting everywhere) prior to establishment of the nominal loop operating conditions. This document describes the operation of these TCLs and the results obtained.

2. EXPERIMENTAL

2.1 LOOP FABRICATION

A schematic of the TCL design is shown in Fig. 1. Each TCL in this study was fabricated of mill annealed alloy 316L SS seamless tubing (25.4 mm ID, 1.8 mm wall) with the composition shown in Table 1. The thermocouple wells, which protruded about halfway into the flow channel, were also seamless, mill annealed 316L SS tubing (6.4 mm OD, 0.7 mm wall). The valves and a few other metallic accessories (connectors, transfer lines, etc.) were 316 or 316L SS. [This design is identical to previous TCL tests with 316L.⁶]

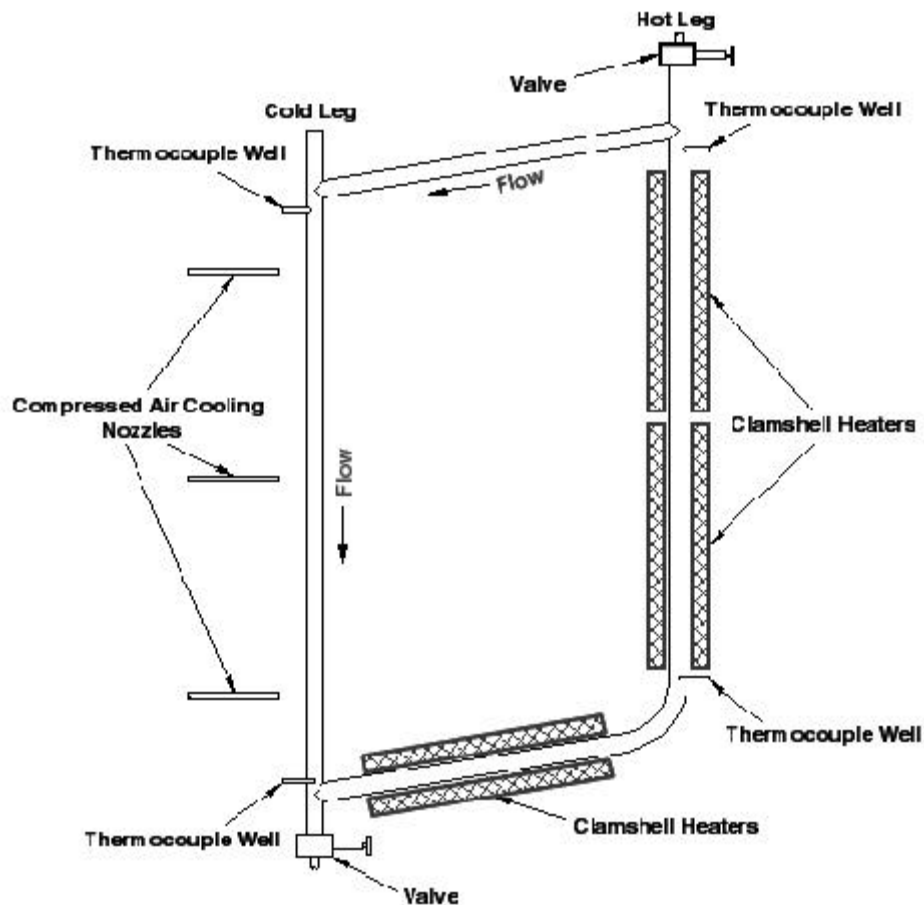


Fig. 1. Schematic of the thermal convection loop design. The distance between thermocouple wells on each vertical section is about 70 cm in the actual loop, and the vertical sections are separated by about 45 cm.

Table 1. Composition of alloy 316L SS TCL tubing and specimens. Data from mill certification for each material, given in weight percent.

Element	316L tubing	316L specimens	316LN specimens
C	0.013	0.018	0.009
Cb	0.17	----	----
Co	----	----	0.16
Cr	16.75	16.10	16.31
Cu	0.30	0.29	0.23
Fe	balance	balance	balance
Mn	1.84	1.73	1.75
Mo	2.12	2.15	2.07
N	0.046	0.030	0.11
Ni	10.19	10.10	10.20
P	0.028	0.028	0.029
S	0.014	0.005	0.002
Si	0.34	0.50	0.39

Each TCL contained a chain of 316L SS specimens in the heated and cooled vertical sections (typically termed the “hot leg” and “cold leg,” respectively). Each specimen chain consisted of 30 rectangular coupons and 2 miniature tensile specimens (see Fig. 2 for specimen dimensions) joined together with a continuous 316L SS wire (about 0.4 mm diameter) via the holes in the corners/ends of each specimen. The end of each wire was welded to the bottom of the respective vertical sections to keep the chains from floating to the top of the Hg, and positioned such that the top and bottom of the chain corresponded approximately to the thermocouple well positions in each leg. To minimize specimen movement relative to each other and facilitate close spacing, adjacent rectangular coupons were interlocked via the small notch at each end of the specimen; thus, alternating coupons were turned 90° relative to each other.

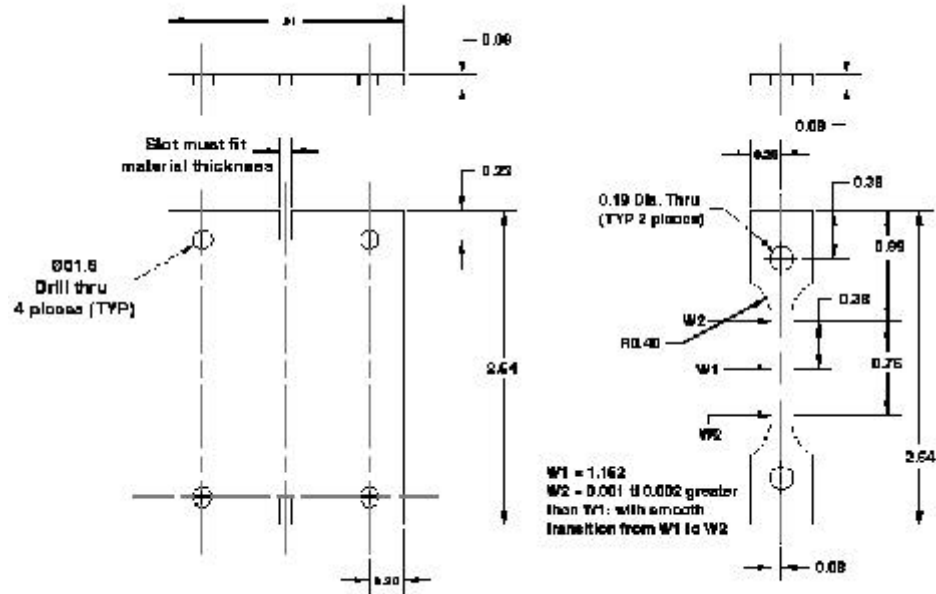


Fig. 2. Dimensions (in cm) of rectangular coupons and miniature tensile specimens.

In addition to a number of standard surface-ground/mill-annealed specimens in each chain, specimens representing several other conditions were included for comparison. These specimen variations included (along with relative position in the chain; Position 1 at the top):

- polished specimens; these were polished on one of their large faces through 1 μm alumina paste (Positions 4 and 19 in each leg),
- oxidized specimens; these were heated in air for 2 h at 900°C and slow cooled in the furnace; (Positions 1 and 16 in each leg),
- gold-coated specimens; one side of these coupons was sputtered with Ar^+ in a high-vacuum chamber to remove the oxide film, then sputter-coated with gold to a thickness of approximately 0.25 μm in the same chamber without readmitting air (Position 3 in hot leg and Position 18 in cold leg),
- etched specimens; these coupons were immersed in a 40% reagent grade sulfuric acid solution at 70°C for six minutes – the black “smut” that formed on the specimens was removed by ultrasonic cleaning in acetone (Positions 10 and 25 in each leg),

- simulated radiation damage specimens; these specimens were bombarded on one side with 1×10^{17} Fe/cm² at 30 keV and 100°C to a calculated 43 dpa at the surface (Positions 6 and 21 in each leg),
- sensitized specimens; these were heated 20 h at 650°C in vacuum and lightly pickled to remove a very thin surface tarnish (Positions 8 and 23 in each leg),
- welded specimens; an electron beam welding device was used to generate an autogenous weld pad in the central two-thirds of both large faces of the specimens (Positions 12 and 27 in each leg),
- miniature tensile specimens; these were mill-annealed with the same composition and surface finish as the rectangular coupons except for the edges, which were cut by the electro-discharge machining technique (Positions 5 and 28 in each leg), and
- 316LN specimens; these were standard surface-ground/mill annealed coupons, but doped with nitrogen and having a slightly different bulk composition than the 316L used for the other specimens (Positions 14 and 30 in each leg).

The specimens in each chain were individually numbered, cleaned ultrasonically in acetone, and weighed (before and after each “treatment”) prior to assembly of the chain. All specimens were handled with gloves and tweezers during the stacking and wiring activities.

Prior to fabrication of the TCLs, the ID of the 316L tubing was mechanically and chemically cleaned to remove fabrication debris and make the ID surface as smooth and uniform as possible. Mechanical cleaning of the tube ID was accomplished with a 302 SS bristle brush attached to an extended rod and powered by a standard hand drill. Subsequently, tube sections were capped with rubber stoppers and each tube section was filled with a pickling solution (10% nitric acid and 3% hydrofluoric acid in water, ambient) for about 10 minutes at room temperature. Following this treatment, the required cutting and bending of the tubes (tubing filled with a very soft Bi-In-Sn alloy to prevent tube collapse) was performed and the tubing was rinsed with alcohol and air-dried.

Following fabrication, specimen placement, and final assembly, the loops were filled with methanol as a final leak check. Unlike the initial 316L TCLs,⁶ no steam treatment was included in the loop preparation.

2.2 FILLING WITH MERCURY

Each loop was alternately evacuated (internal pressure of a few microns of mercury) and filled with helium several times. Subsequently, the loop was evacuated and filled with mercury from the reservoir at the top (the ullage of which was also evacuated/purged with helium).

Approximately one atmosphere of helium was used as a cover gas for the mercury in the loop. The loop was warmed to near operating temperature and the excess mercury (expanded above fill line at room temperature) was drained off through a side arm of the loop.

Virgin mercury from the same batch as that used for the original 316L SS loops⁶ was used for these experiments. Standard chemical analysis of representative samples indicated the Hg was quite pure, containing only about 85 ppb Ag and 100 ppb Si above detection limits. Immediately prior to use in the loops, the Hg was "filtered" through cheesecloth to remove the small amount of residual debris (oxides) floating on the surface of the Hg.

2.3 LOOP OPERATION

Generally, the heat-up and operation of the TCLs was identical to that reported previously⁶ for 316L SS TCLs. Clamshell-type furnaces were placed on the vertical leg (two furnaces) and on the near-horizontal lower portion of the loop (one furnace) for long term operation. The control temperature of the lower furnace was kept somewhat below the temperature of those on the vertical hot leg to help maintain the mercury flow pattern. The vertical section of each cold leg was cooled by compressed air delivered from three roughly equispaced copper tubes with outlets placed close to the outer loop surface and an array of small fans providing air movement across the entire cold leg. After a day or so of furnace temperature and airflow adjustments, the temperature at each thermocouple well position and the mercury flow rate became quite stable. The temperature at each location varied only by about $\pm 2^\circ\text{C}$ over the entire 2000 h uninterrupted duration of the experiments. Table 2 compares temperatures at each thermowell for these TCLs with the same data for TCL 1.⁶

During start-up, one of the TCLs described here was intentionally treated somewhat differently. Rather than standard initiation of heating on the hot leg and concurrent cooling of the cold leg to establish Hg flow, the entire TCL 5 was fitted with clamshell furnaces and heated to 310°C for about 36 h. After the soak at 310°C (intended to aid wetting), the furnaces on the cold leg and upper horizontal section were removed and airflow to the cold leg was initiated. The pre-operational soak at 310°C was not attempted on TCL 6; rather, TCL 6 was considered an attempt to "duplicate" the result of the initial 316L TCL (Loop 1 in Ref. 6). The remainder of loop operation was identical for both TCLs.

Table 2. Nominal temperatures at each “corner” of the thermal convection loops described here along with equivalent data for TCL 1 (a previous 316L TCL). Approximately a $\pm 2/C$ drift over the duration of the experiment was measured at each location.

	TCL 5	TCL 6	TCL 1
Bottom of hot leg	269/C	274/C	268/C
Top of hot leg	306/C	305/C	305/C
Top of cold leg	284/C	286/C	280/C
Bottom of cold leg	245/C	238/C	242/C
Nominal temperature gradient (maximum to minimum)	61/C	67/C	63/C

The flow rate of the mercury inside the loop was determined via a localized “temperature spike” test. In this test, a propane torch was used to heat a small area in the middle of the roughly horizontal section at the top of the loop for about 15 seconds. The time required for the resultant temperature “spike” to reach each thermocouple in sequence around the loop along with the distance between thermocouples was used to estimate the velocity of the mercury. The mercury flow rate was found to be approximately constant at 1.2 m/min in each loop over the duration of the experiment in each loop.

3. RESULTS AND DISCUSSION

3.1 INTRODUCTION

Loop 5 and Loop 6 were both terminated after 2000 h of uninterrupted operation. After about an hour of cooling, the mercury was drained from each loop via the valve at the bottom of the cold leg. In each case, the post-test mercury appeared bright and shiny – essentially identical to its appearance when poured into the loop.

Handling as gently as possible (to avoid excessive jostling/vibration), each loop was subsequently cut (dry, using a tubing cutter and a jeweler's saw) in strategic locations to free the specimen chains in each of the vertical legs. The appearance of the post-test coupons (no cleaning; effort made not to disturb specimen surfaces) was documented photographically, and representative examples will be discussed in the paragraphs that follow for exposure of each type of coupon.

3.2 NOMINAL 316L SPECIMENS

In these TCL experiments, the role of the nominal (mill-annealed, surface ground) 316L coupons was two-fold: first, to function as near-neighbor “control” specimens to other specimens with a range of surface and structure variables and, second, to permit a comparison with previous coupon data from similar TCL experiments. Based on visual assessment of the post-test coupons, none of the nominal 316L specimens exhibited more than very minor wetting (small areas with Hg films or beads clinging to the surface) and none lost weight greater than potential scatter in the measurements. A few specimens exhibited a small weight gain (0.2-1.0 mg) but no pattern regarding wetting, discoloration, or metallographic features could be associated with this behavior.

Consistent with little or no weight change, post-test metallographic cross sections of the standard coupons revealed essentially no change in the surface roughness compared to the original condition. However, isolated locations were observed (particularly on coupons exposed to the highest temperatures) with a microstructure that indicated an interaction between the stainless steel and the Hg. Perhaps the most prolific occurrence was for Coupon 5H2 (near top of the hot leg in Loop 5). A representative cross section is shown in Fig. 3, and it reveals a porous and attacked structure at the surface compared to the original coupon condition (which exhibited only minor relief due to the surface ground finish). This structure is similar to that observed on coupons removed from Loop 1 (in which wetting and interaction with Hg was also observed⁶). In

localized areas where the porous structure forms (not completely uniform), maximum penetration is only 5-10 μm in 2000 h.

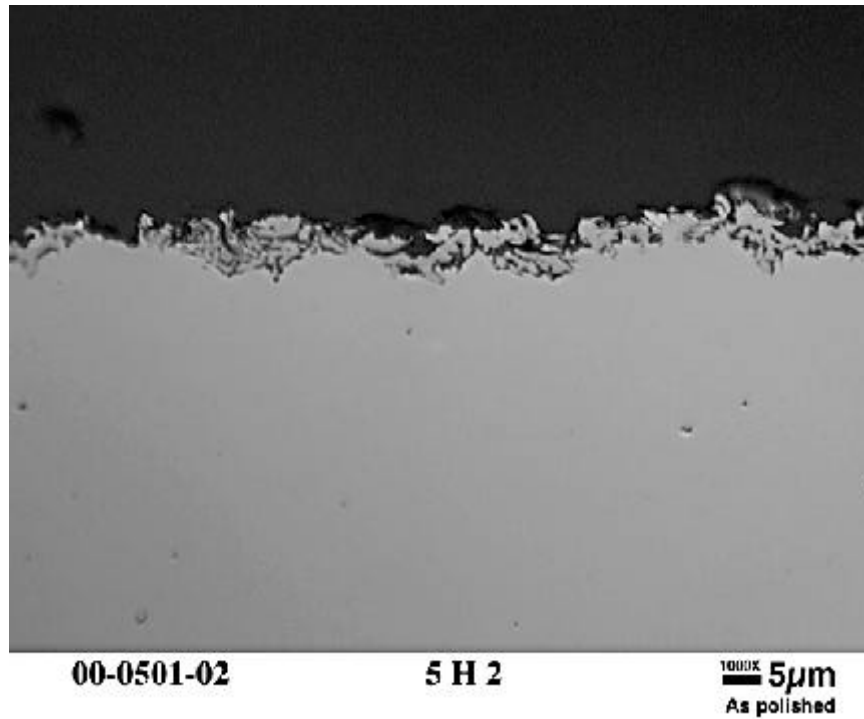


Fig. 3 . Post-test cross section of Coupon 5H2 in the as-polished condition. This coupon was exposed near the top of the hot leg in Loop 5 at a temperature of about 304°C. The surface which was wetted by the Hg has become porous. Most areas of the coupon surface reveal less surface porosity than shown in this photomicrograph.

Electron microprobe analysis of the porous surface reveals that the near surface regions (between the surface exposed to Hg and the extent of maximum penetration of the porous region) have been leached of essentially all of the Ni and about 75% of the Cr. The composition gradient in this region is very steep, however, as immediately adjacent to the porous regions (0.5 μm on the bulk side of the reaction interface), the composition is indistinguishable from that observed in the center of the specimen and from the original composition. Figure 4 is representative of this observation, and it shows that for region 1 (in the porous structure) the Ni and Cr are significantly depleted. Region 2, just on the bulk side of the interface, reveals almost no Ni or Cr depletion. Region 3, which is an isolated region in this area apparently free from attack, exhibits the same composition as the center of the specimen.

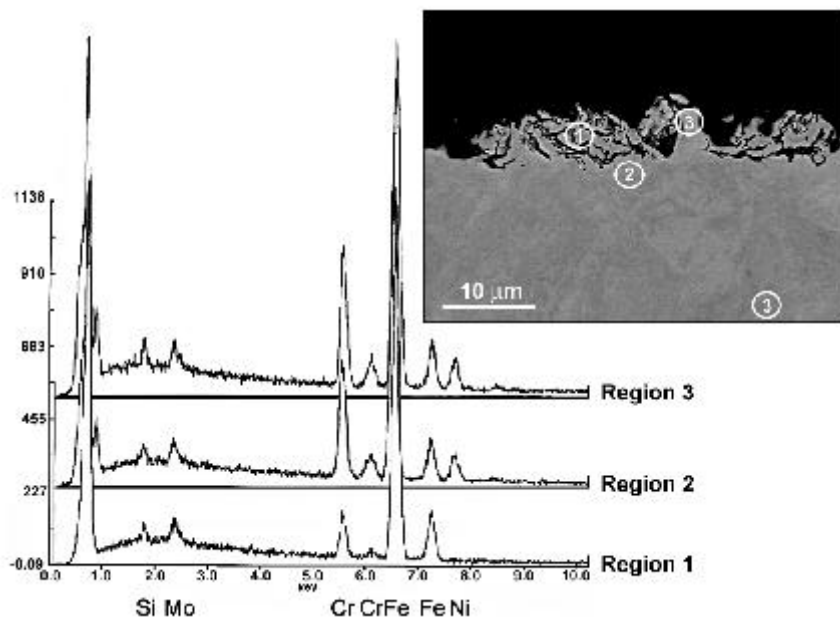


Fig. 4 . Representative backscattered electron image and microprobe results from labeled areas from Coupon 5H2 (annealed 316L). Note that the peak associated with Ni is essentially absent from the surface scan (Region 1) and the peaks associated with Cr are significantly reduced.

These observations indicate that, at least in sporadic locations, the Hg chemically wet the surface of the nominal coupons leading to leaching of Ni and Cr similar to that observed in Loop 1.⁶ However, for reasons that are not clear, the extent of the areas wet by Hg was relatively limited. In areas where the maximum attack is observed, however, the depth of penetration is very modest and corresponds to only 20-50 $\mu\text{m}/\text{y}$ (about 1-2 mils/y).

3.3 SPECIMENS COATED WITH GOLD

Since an air-formed passive film on stainless steel can be a significant barrier to chemical wetting by Hg, a small number of specimens were coated on one side with gold in an attempt to promote wetting of the stainless steel. In principle, sputtering of the stainless steel surface in a high vacuum chamber with Ar^+ ions removed the oxide film from the surface of the material. Following sputtering to clean the surface, with the specimen still in the same chamber free from exposure to air, the coupon was rotated to a position in which a thin film of gold could be sputter-coated onto the exposed stainless steel surface. The gold-coated specimens could then be handled in air (removed from the chamber, added to the coupon chain, exposed to Hg) while maintaining the oxide-free nature of the surface beneath the gold. By depositing the gold in this

fashion – directly onto an atomically cleaned surface rather than onto an oxide – it was expected that upon exposure, Hg would rapidly amalgamate the Au and place a large area of oxide-free stainless steel surface into direct contact with Hg.

The sputter-coating process to deposit gold was performed for the same length of time for each specimen. However, weight change measurements following the cleaning and gold deposition activity (Table 3) indicate the process was not particularly uniform. Using the area of one face of the coupon and the mass of gold added, the average thickness of the gold film varies among the coupons from about 0.1 μm to about 0.4 μm . It is not apparent from the weight change data in Table 3 that the thickness of the gold deposit had any direct influence on the coupon interaction with Hg, as specimens with the greatest and least amount of gold coating are both “mid-range” results in terms of overall weight change in the TCL.

Table 3. Weight change data for 316L specimens coated with gold on one side.

Coupon ^a	Mass of gold (mg) applied	Exposure temperature ($^{\circ}\text{C}$) ^b	Weight change (mg) above/beyond loss of gold ^c
5H3	0.76	303	-5.35
5C18	4.87	263	-4.86
6H3	2.25	303	-3.86
6C18	1.84	261	-6.36

^a Coupon designation gives the loop number (5 or 6), whether it was in the hot leg or cold leg (H or C), followed by the coupon position number.

^bExposure temperature estimated by linear extrapolation of temperatures between thermowells.

^c The weight change for each coupon was calculated by subtracting the post-test weight (after removing residual Hg) from the original coupon weight (before gold coating).

Table 3 also reveals that the Hg temperature (specimen position in the loop) does not strongly influence total weight change in the TCL exposure. In particular, note that the highest weight change occurred for the specimen exposed at the lowest Hg temperature (261 $^{\circ}\text{C}$).

Based on the post-test appearance of the coupons, the side coated with gold experienced a significant degree of wetting compared to the uncoated side. Figure 5 is a representative example of this observation: in each case, a somewhat tenacious film of Hg remained on the side formerly coated with gold, while the uncoated side was essentially devoid of visible Hg. During gold-coating, the side of the coupon not being coated was supported on a circular stand. The area

completely masked by the stand is evident by the relatively shiny, circular area in the center of the back of the coupon. At the extreme edges of the back, the coupon reveals no apparent wetting but some interaction with Hg has darkened the surface luster considerably. The reason for the dark coloration is not clear, but it perhaps relates to the deposit of a thin, irregular gold film which generated only irregular interaction with Hg. However, other coupons (not associated with the gold-coating process) occasionally reveal dark discoloration, which may suggest a mercury sulfide constituent. After Hg was wiped from the wetted surface and the coupons cleaned in an ultrasonic bath of acetone, the formerly wetted (gold-coated) surface revealed a dull gray luster and a slightly roughened or even lightly pitted appearance.

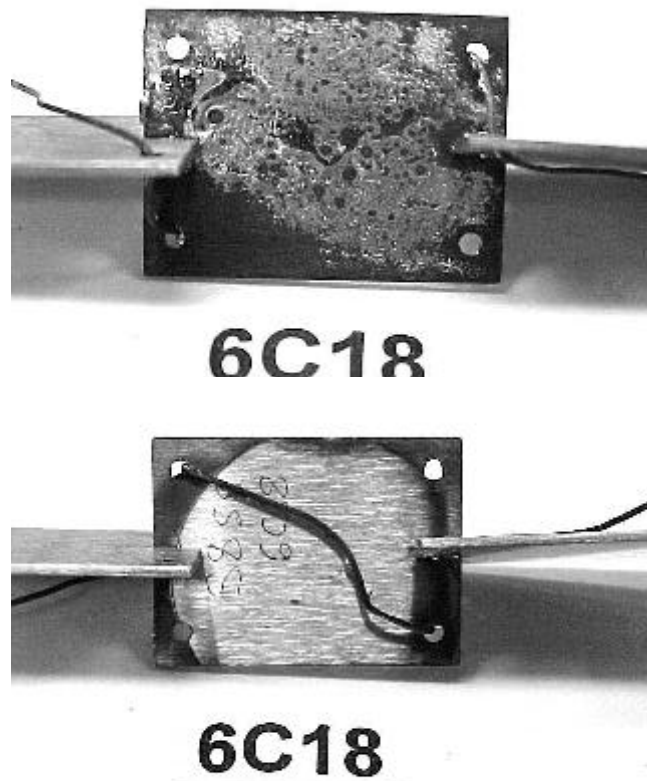


Fig. 5. Post-test appearance of Specimen 6C18, which was gold coated on one side (top photo) and was protected from gold coating on the opposite side by a circular support stand (bottom photo). The side formerly coated with gold retains no gold coloration but residual Hg clings to large portions of the surface with a low contact angle. The majority of the opposite side, protected from gold coating, is essentially unaffected by exposure to Hg.

It is interesting that any disruption of the wetted surface at room temperature, such as lightly wiping to remove bulk Hg, immediately rendered the coupon unable to “re-wet” upon dipping into ambient Hg. Even extended exposure to air with no mechanical disturbance tended to cause beading of the Hg and loss of wetting.

Post-test metallographic cross sections of the gold-coated coupons reveal a significant increase in surface roughness on the coated side. Figure 6 is representative of this observation and it shows at least 15 μm of penetration into the originally uniform surface. Relatively little of the “porous structure” similar to that discussed in relation to Figs. 3 and 4 was observed on the coated specimens, even though the weight change on these coupons was even larger than that for previous coupons (Loop 1)⁶ in which the porous surface was readily detected. Electron microprobe analysis of cross sections of the gold-coated specimens revealed no trace of residual gold, and Ni and Cr depletion only in areas in which the porous structure is evident (always the side that had been coated with gold). In areas such as that depicted in Fig. 6, there was no change in composition compared to the bulk. It would appear that Hg attack was sufficiently aggressive on the gold-coated side of the coupon that small pieces of the porous surface were completely dissolved or perhaps dislodged to create the observed surface roughness and weight loss. Nevertheless, the maximum extent of penetration still corresponds to only about 60-70 $\mu\text{m}/\text{y}$ (<3 mils/y) for the conditions examined in this TCL.

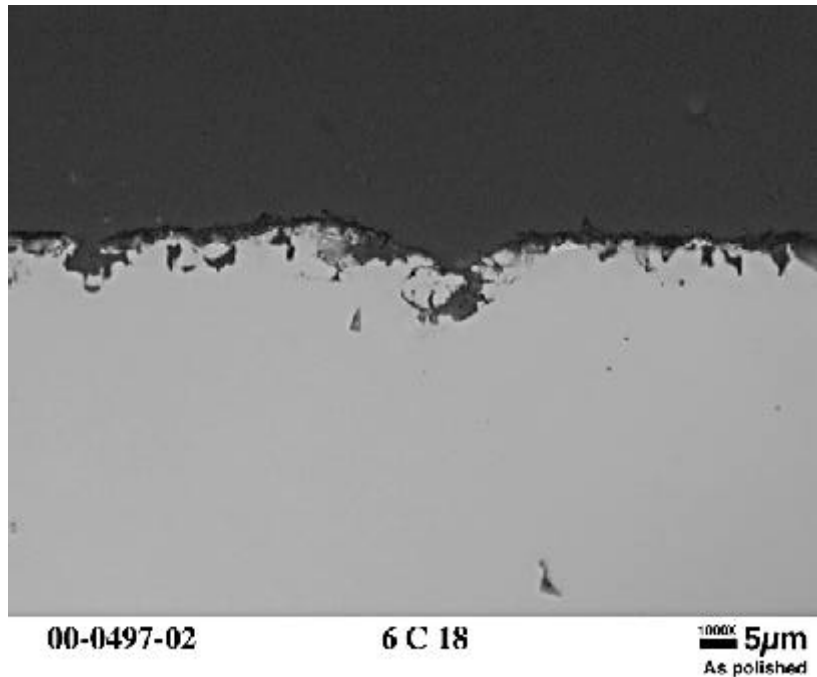


Fig. 6. As-polished cross section of Specimen 6C18 on the side formerly coated with gold. Note the surface roughness and irregular penetration.

A crude comparison of coupon weight change data for the gold-coated coupons with coupons showing the maximum weight change in the original 316L TCL⁶ can be performed as follows. Based on visual appearance and metallographic examination, most of the interaction on the gold-coated specimen occurred on only one-half the total specimen area (gold-coated side). To compare with results from TCL 1,⁶ attack of this magnitude must be extrapolated to both sides of the coupon and to 5000 h exposure rather than 2000 h. In round numbers, then, the average weight loss of the gold-coated coupons (5.1 mg) can be multiplied by 2 to account for area and by 2.5 to account for duration. This estimate yields an average weight loss of 25.5 mg per coupon, or about 60% greater than the maximum weight loss observed in Loop 1.⁶ This crude comparison suggests that the gold coating facilitated greater weight loss, perhaps by decreasing the time required for chemical wetting and leaching to begin. In any case, the total extent of attack for the gold-coated specimens corresponds to about 60-70 $\mu\text{m}/\text{y}$ (<3 mil/y) based on maximum penetration.

3.4 OXIDIZED SPECIMENS

If an air-formed passive film on stainless steel is a significant barrier to chemical wetting by Hg, a specimen with a thick air-formed film might be expected to be immune to attack by Hg under the conditions being investigated. To test the concept, standard 316L coupons were heated in lab air for 2 h at 900°C and then slow cooled in the furnace. A uniform golden-brown tint was developed on each coupon, and the weight of each increased consistently by about 0.7 mg as a result of the thick oxide formation.

Specimens so oxidized were placed at Positions 1 (extreme top, highest temperature) and 16 on the coupon chains in each hot leg and cold leg. Following removal from the TCLs, visual examination of all eight specimens revealed no obvious change in the golden brown tint on any of the specimens, and only one specimen (6H1) revealed any hint of wetting (a few tiny beads of Hg clinging to the surface on one side).

Weight change analysis indicates essentially no post-oxidation change among these coupons and little or no deviation in weight change compared to the “nominal” 316L specimens located nearby on the chain. With the exception of the same specimen that exhibited tiny beads of Hg clinging to the surface (6H1), the average weight change among the other seven specimens was near the level of variability of the measurement itself (about $\pm 0.03\text{mg}$) and, for practical purposes, is considered unchanged from the pre-test weight. Specimen 6H1 experienced a slightly higher weight gain (0.7 mg) and, despite attempts to clean the specimen, this could relate to small amounts of Hg retained in/on the film. In any case, the relatively heavy oxide film seems

to render the 316L immune to corrosion/attack for the relatively low flow and irradiation-free conditions examined here.

3.5 POLISHED SPECIMENS

The typical surface roughness of the standard 316L coupons used in these experiments corresponds to about 0.8 μm (32 microinches). To examine the potential influence of surface roughness, one side of a limited number of specimens was polished through 1 μm alumina paste to a mirror finish. Specimens with one side polished were included in the specimen chains at Position 4 (near the top) and Position 19 in each leg for each loop.

Post-test observation of the specimens polished on one side revealed minor wetting (based on areas in which Hg seemed to cling to the surface with a low contact angle) on the specimens near the top of each of the hot leg (exposed at temperature near 300°C) but not on any of the other six specimens. Figure 7 shows an example (Specimen 6H4) of a specimen apparently wet by Hg on the polished side and not at all on the opposite side.

Weight loss analysis for the polished specimens indicates a slight tendency to lose weight; only one specimen revealed a very modest weight gain. Specimen 5H4 lost the maximum weight among the polished specimens (0.29 mg) but this corresponds to extremely minor general attack over 2000 h. Figure 8 confirms the limited extent of attack for Specimen 5H4. Note, however, that even the very limited attack is not uniform over the specimen surface, perhaps indicating only localized areas of chemical wetting on the specimen surface. Compared to weight changes on nearby specimens and to specimens at similar positions in Loop 1,⁶ it appears that polishing to reduce surface roughness neither significantly enhances or inhibits wetting for the conditions examined in these TCLs.

3.6 SIMULATED RADIATION DAMAGE SPECIMENS

In the SNS target, areas near the window will be exposed to high levels of radiation. In particular, the surface exposed to Hg will be atomically mixed (literally “scrambled”) by neutron damage and the associated knock-on particle activity. Either the passive film might be destroyed in this process (permitting direct interaction of the oxide-free surface with Hg) or possibly the film that forms after irradiation would respond differently to wetting/attack by Hg than a nominal air-formed film. To investigate the latter possibility (without actually placing Hg and specimens in-beam), one side of a small number of specimens was irradiated on one side with 1×10^{17} Fe/cm² at 30 keV and 100°C to a calculated 43 dpa at the surface. The dose was applied in a roughly circular area that covered most of one major face of each coupon so treated. The iron-doped

specimens were placed at Positions 6 and 21 in each leg of each loop. Iron was selected for bombarding the surface as it could be used to generate appropriate displacement damage without a significant surface composition change or radioactivity.

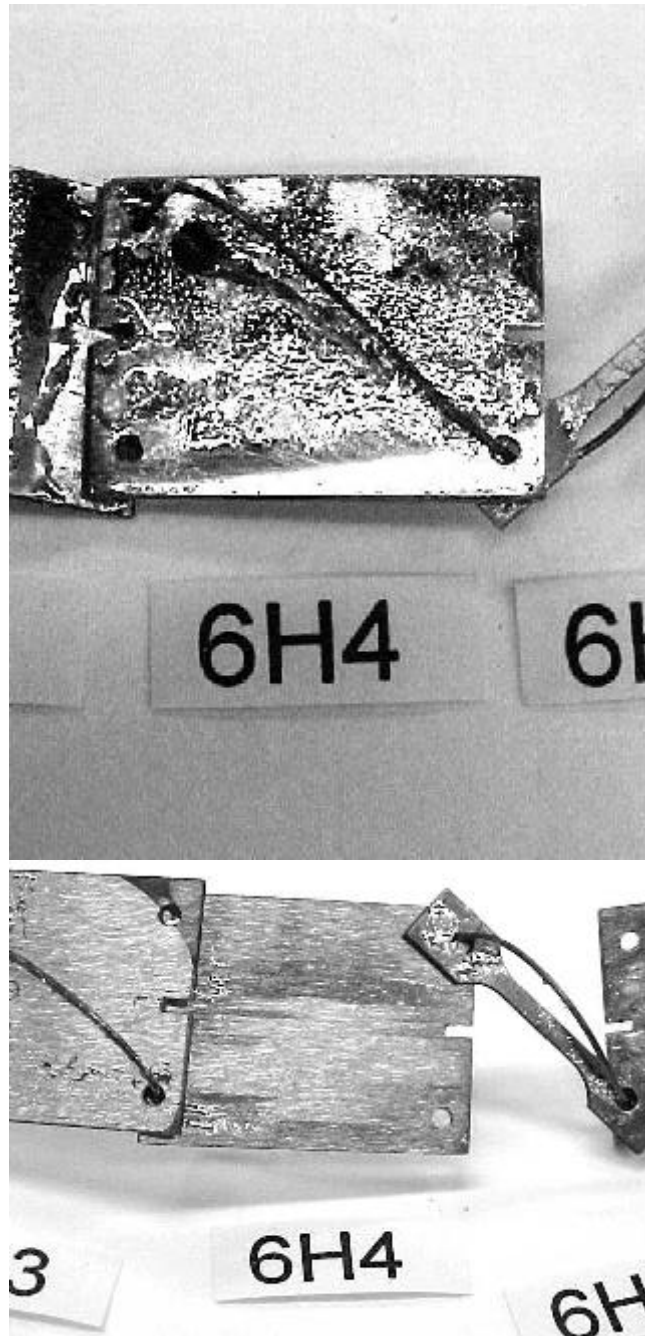


Fig. 7. Post-test appearance of Specimen 6H4, which was polished on one side (top photo) and in the surface ground condition on the opposite side (bottom photo). Note significant clinging Hg on the polished side (film of Hg with low contact angle) but little Hg and only minor discoloration on the unpolished side.

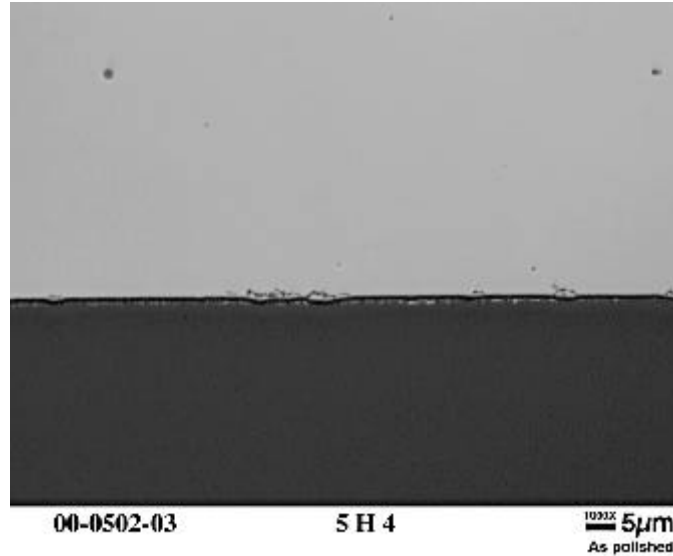


Fig. 8. As-polished cross section of Coupon 5H4, which was polished on the side shown. Note that the surface is generally smooth and only limited penetration is indicated.

Post-test visual examination revealed little change in appearance as a result of 2000 h exposure to Hg. Minor exceptions include a few streaks of Hg clinging to Specimen 6H6, and Specimens 6C6 and 6C21 which exhibited a pattern similar to that shown in Fig. 9. The interaction between the Hg and stainless steel surface that generates this pattern is unknown, but the darkening clearly delineates areas experiencing a high dpa prior to exposure to Hg.

Compared to the weight change of specimens nearby in the coupon chain, only 6H6 and 6C6 exhibited a significant weight change (-0.44 mg and -0.95 mg, respectively). These are very modest weight changes in terms of damage/penetration in the coupon. A representative example is shown in Fig. 10, which is a cross section of Specimen 6C6. None of the other specimens with 43 dpa at the surface due to iron bombardment revealed a significant weight or appearance change compared to the near-neighbors on the specimen chain.

3.7 SENSITIZED SPECIMENS

In a solution treated (sometimes called annealed) austenitic stainless steel such as 316/316L, the material has been quenched from a high temperature (about 1100°C) in order to keep alloying elements uniformly distributed and, in particular, retain the carbon content in solution. If such material is reheated into the temperature range of 500-900°C (typically due to welding or stress relief treatments, or potentially an elevated service temperature), chromium carbides tend to form on grain boundaries in the material. These precipitates are very rich in

chromium and tend to significantly deplete the surrounding matrix in chromium. As a result, the regions adjacent to grain boundaries may be sufficiently depleted in Cr that passivity cannot be maintained in a number of environments (leading to intergranular corrosion along these paths). Since previous work⁶ showed that Hg has some affinity for leaching Cr from 316L stainless steel wetted by Hg, the potential for attack on a Cr-rich phase such as chromium carbides was deemed worthy of consideration. [In addition, enhanced wetting of Cr-depleted areas is a possibility.] While “L” grades of stainless steel are generally resistant to formation of continuous networks of grain boundary precipitate, relatively long heat treatments in the critical temperature range can cause these carbides to form, and a material in this condition is termed sensitized.

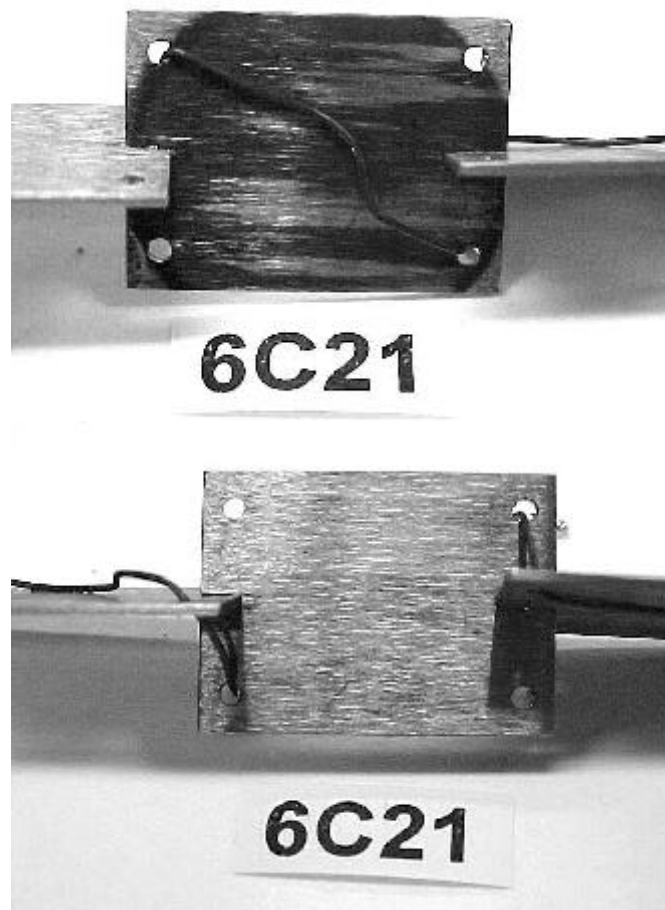


Fig. 9. Post-test appearance of Specimen 6C21, which was implanted with Fe to simulate irradiation damage on one side (top photo, circular region) and was protected from implantation on the other side (bottom photo). No Hg beads were observed to cling to this specimen.

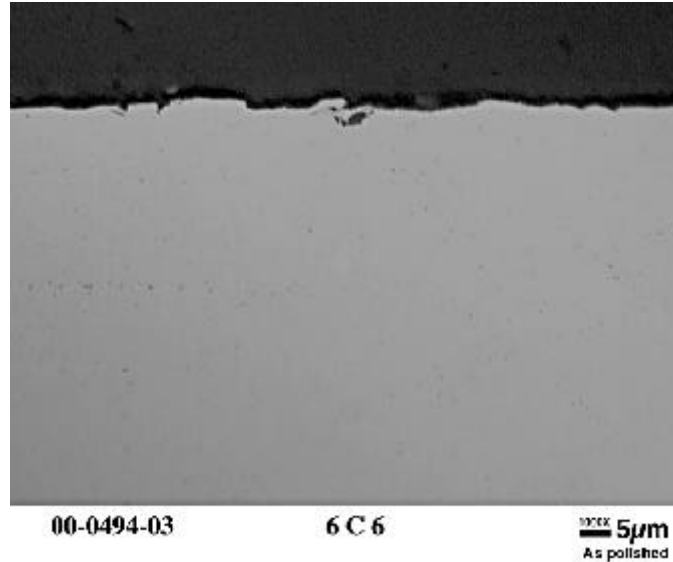


Fig. 10. As-polished cross section of Coupon 6C6, which was implanted with Fe to simulate irradiation damage on the side shown. The extent of penetration is both irregular and very shallow.

To examine a sensitized microstructure in Hg, the standard 316L coupons were heat treated for 20 h at 650°C in vacuum to limit oxidation of the surface. After heat treatment, the specimens were lightly pickled to remove the very light “tint” resulting from heat treatment in less than a perfect vacuum. [The pickling treatment generated a surface only slightly dull gray compared to the nominal shiny gray surface of the standard specimens.] Sensitized specimens were placed at Positions 8 and 23 in each leg of each loop.

None of the sensitized specimens revealed a weight change significantly different from its near-neighbor standard coupons and no changes had an absolute value greater than 0.1 mg. However, all of the sensitized specimens revealed areas in which the specimen had dark film/stain, and those at the top of each cold leg exhibited minor wetting (clinging of small Hg beads). It is not clear if the darkened surface is related to a residue of the pickling treatment (20% nitric acid plus 3% hydrofluoric acid, 5 minutes at room temperature, rinse in water, dry with acetone rinse) or some aspect of the sensitizing treatment. An example of the dark, streaky surface of the sensitized specimens appears in Fig. 11. No surface roughening or penetration was observed in the post-test cross sections of sensitized specimens.

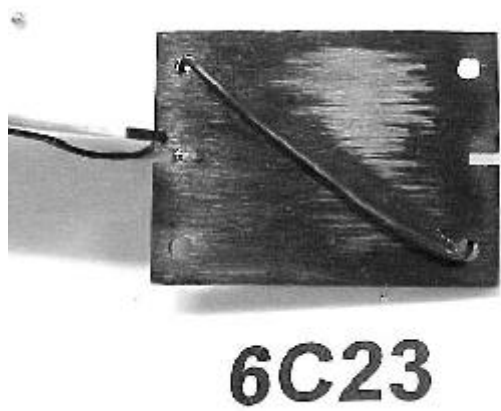


Fig. 11. Post-test appearance of Specimen 6C23, which was sensitized (20 h at 650°C) prior to the test. A dark film adheres to most of this specimen (but not to adjacent specimens in the chain). Tiny beads of Hg can be observed clinging to the specimen, particularly near the holes in the coupon.

3.8 ETCHED SPECIMENS

Etching in 40% sulfuric acid at 70°C is an aggressive treatment used for plating baths and related activities to remove the passive film from many stainless steels. After a few seconds exposure to this treatment, typical stainless steel surfaces violently evolve hydrogen from the surface (reduction of the oxide film) and accumulate a dark, lightly adherent smut that is a combination of several iron sulfides and related corrosion products. Although this treatment previously provided only sporadic success in generating apparent wetting/clinging of Hg on stainless steel surfaces,⁵ it was utilized here to further gauge its utility as an aid to wetting in long term Hg exposure tests. Specimens were soaked six minutes in the above solution, then rinsed and ultrasonically cleaned in acetone to remove the smut (leaving a light golden brown tarnish) before being placed at Positions 10 and 25 in each leg of each loop.

Post-test examination of the etched specimens indicates very little or no change in appearance in that the tarnish film appeared unaffected by exposure to Hg, and only minor indications of wetting (a few spots of clinging Hg beads) were observed on two of the etched coupons. No coupons lost weight, and none of the very small weight gains were significantly different than similar results for near-neighbor specimens. It appears the etching procedure (at least as employed here) is not effective for improving wetting and has no effect on the performance of 316L in the Hg TCL conditions that were used in this test.

3.9 WELDED SPECIMENS

Welding of 316L stainless steel will change the local composition, structure, and surface roughness of target components. The local composition could change as a result of several factors, including volatilization of Cr and/or tarnish film formation during high temperature excursions, introduction of segregation and formation of second phases, potential sensitization, and introduction of filler metal materials. Further, welding is expected to increase surface roughness by adding surface relief, pores, and other irregularities.

To examine some of these possibilities, the standard 316L coupon specimens were modified by creating an autogenous weld pad in the central portion of both sides with an electron beam welder. Weld penetration was only minor, but a significant area was created with a cast austenitic structure (very little or no ferrite formation). Two weld specimens were placed in each leg of each loop (Positions 12 and 27).

In several instances, various degrees of apparent wetting (residual Hg clinging to the surface with a low contact angle) were observed associated with the weld pads. Representative examples are shown in Fig. 12. Despite the apparent inclination toward wetting, none of the welded specimens revealed a weight loss and only one revealed a weight gain larger than the scatter of the measurement. Since none of the weight changes were significantly different from near-neighbor specimens, it appears that the weld structure is not detrimental to the performance of 316L in Hg for the conditions examined in this TCL.

3.10 316LN SPECIMENS

At present, some consideration is being given to selection of a nitrogen-doped 316L (termed 316LN) for the target containment material and possibly the proton beam window. Nitrogen additions to many stainless steels are known to increase strength and improve other mechanical properties as well as improve corrosion resistance in many aqueous environments.^{8,9} In addition to increased strength, another potential advantage of 316LN is that it exhibits superior post-irradiation ductility compared to standard grades of 316 SS.¹⁰ The principle advantage of increased strength is that thinner sections in the window area of the target can be used (to minimize in-wall heating, loss of beam intensity, and improve cooling). Type 316LN specimens have already been incorporated in irradiation¹⁰ and fatigue¹¹ studies for the SNS, and specimens from the same heat of material (see composition in Table 1) have been included in these compatibility studies to evaluate 316LN compatibility with Hg. Specimens of 316LN in the mill annealed (solution treated) condition were placed at Positions 14 and 30 in each leg of each loop.

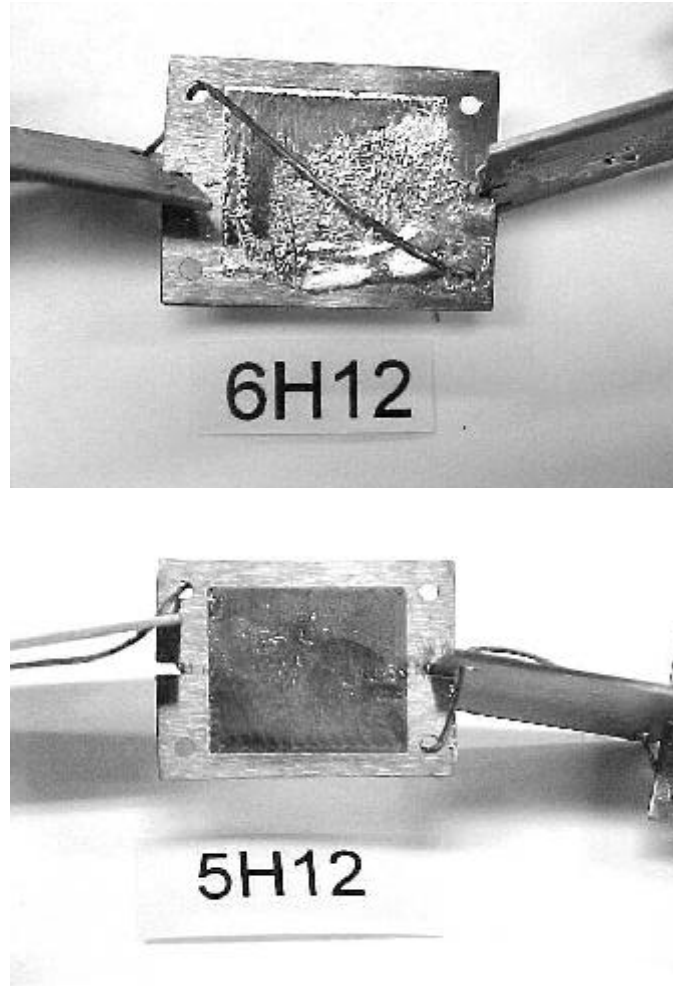


Fig. 12. Post-test appearance of Coupons 6H12 (top) and 5H12 (bottom) indicating the range of Hg wetting associated with the weld pad on each coupon. The apparent “darkness” of the weld pad in the center of each coupon is an artifact of the relatively rough surface as opposed to actual discoloration. Coupon 6H12 has quite a lot of clinging Hg where Coupon 5H12 (exposed at the same temperature) has almost none.

Seven of eight 316LN coupons lost a minor amount of weight (about 0.1 mg) while the near-neighbors of these coupons tended to be unchanged in weight. The remaining 316LN coupon (6C30) gained significant weight (0.9 mg) while its nearest neighbors revealed no weight change. All of the 316LN coupons exhibited various degrees of development of a dark “film” on the specimen surface. Figure 13 is representative of this observation on the coupon which exhibited a weight gain. The film is very thin and adherent, but has not been analytically identified.

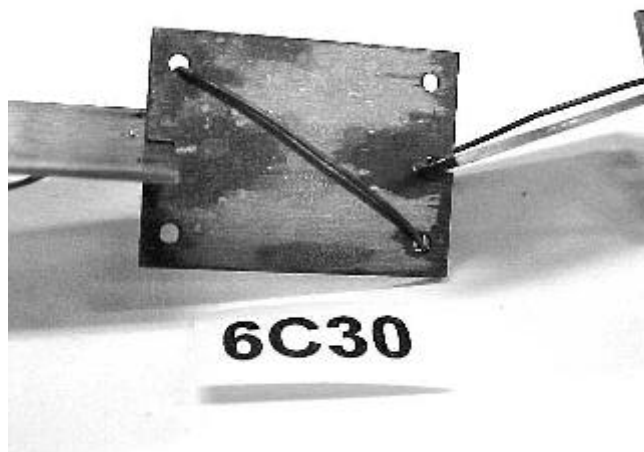


Fig. 13. Post-test appearance of Coupon 6C30, which is type 316LN stainless steel. The irregular dark pattern on the surface was common to these specimens, but little Hg was observed clinging to the surface at any location.

Metallographically, the 316LN coupons reveal sporadic signs of minor attack. An example of this observation appears in Figure 14. The 316LN coupons exhibited more surface relief in the unexposed condition than the 316L coupons (machined somewhat differently at a different shop from the other specimens), but limited attack has occurred. It is not clear if the regions revealing minor attack correspond uniformly to areas of dark film formation, but wetting is required to establish the extent of interaction observed.

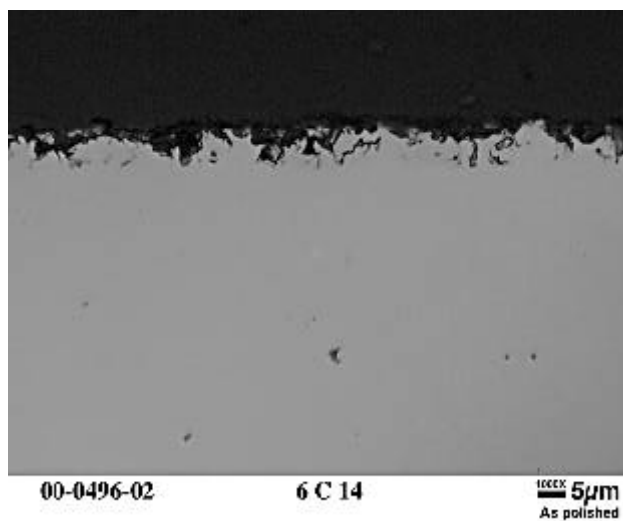


Fig. 14. As-polished cross section of Coupon 6C14 (type 316LN stainless steel). Much of the coupon surface has attack/penetration similar to that shown here (about 5 µm deep).

3.11 TENSILE SPECIMENS

Miniature tensile specimens were included in the TCL coupon chain to permit evaluation of surface effects (if any) on mechanical properties. The tensile specimens were machined from the same heat of 316L as the standard coupons, but the edges of the tensile specimens were cut with electro-discharge machining techniques, which left a rather rough and irregular surface on the edge. These specimens were placed near the top and bottom (Positions 5 and 28) of each leg of each loop.

Only 15 specimens in this entire experiment (total of 128 specimens in the two TCLs) lost weight in magnitude greater than 0.25 mg, and all eight tensile specimens fall into this category. That they did so with about 25% of the surface area of the nominal coupons size is compelling. Metallographically, no particular attack was noted along the specimen cross section (see Fig. 15), but the edges of the specimen were rough and wavy. While the attack on the tensile specimens (particularly on a per unit area basis) is much greater than for the near-neighbor specimens in the chain, it still represents only minor general dissolution/attack corresponding to only about 2-3 $\mu\text{m}/\text{y}$ (0.1 mil/y).

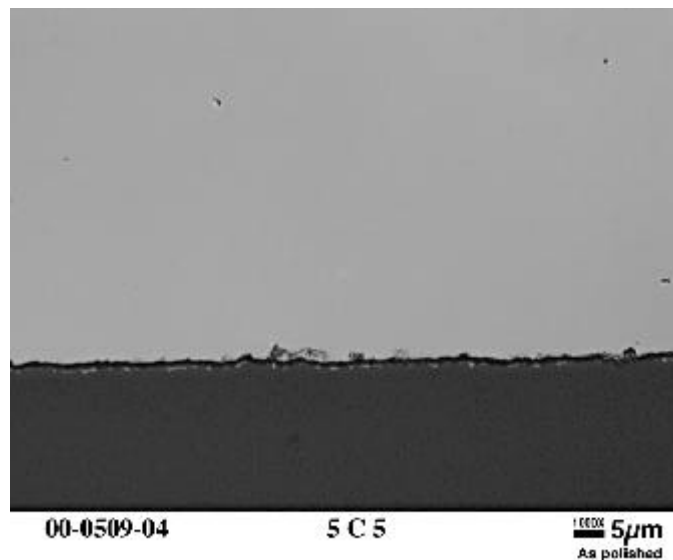


Fig. 15. As-polished cross section of a miniature tensile specimen (5C5) showing only limited penetration/attack at the specimen surface.

It is perhaps significant that relatively greater attack on miniature tensile specimens was also observed previously for alloy 718 in Hg TCLs.⁷ In either case, the behavior is not understood, but it is suspected that the rough and perhaps slightly porous surface generated by the EDM cutting technique possesses a deceptively high surface area and, perhaps, a surface

structure slightly more susceptible to wetting/attack than the base alloy. Due to the very small weight changes and limited extent of attack/penetration observed metallographically, mechanical property data from the tensile specimens was not obtained.

3.12 LOOP PRETREATMENT

Loop 5 was initiated by heating the entire loop with mercury to 310°C for 48 h in an attempt to encourage wetting (all coupons and loop surfaces) prior to establishment of the normal temperature gradient within the loop. Although previous short-term lab tests in air indicated that wetting established at relatively high temperature was not necessarily maintained when the temperature was decreased [unpublished research associated with Ref. 5], long-term exposures to Hg in the absence of air had not been attempted. In contrast, Loop 6 was initiated by heating the hot leg directly from room temperature to the desired set point and cooling the cold leg to establish loop flow conditions. In essence, Loop 6 was an attempt to duplicate the results observed in Loop 1⁶ and to compare this behavior with a loop operated identically with the exception of a high temperature pretreatment in Hg at 310°C.

Coupon appearance (minor wetting and discoloration), weight change (or lack thereof), and metallography (evidence of penetration or other damage) showed no dependence on the pretreatment operation given Loop 5. Further, with the exception of the gold-coated coupons, no specimens in either loop revealed significant interaction with the Hg over the duration of the tests. The only difference in fabrication, cleaning, and operation of Loops 1 and 6 is that Loop 1 received both a brief rinse in trichloroethylene and a brief steam treatment as part of the cleaning just prior to loading with Hg.⁶ The purpose of the additional cleaning in Loop 1 was an attempt to remove residual fabrication debris discovered inside the loop tubing during post-assembly leak checking. The steam treatment (50 psig, two 10 minutes periods) was marginally successful at removing the smut from the tube ID but the coupons were already quite “clean” prior to this treatment. As a result of the difference in coupon behavior between Loops 1 (regular increase in weight loss and uniform attack as the temperature increased above 250°C) and 6 (only sporadic indications of attack at any temperature), it appears that some aspect of the additional cleaning in Loop 1 was instrumental for encouragement of coupon wetting (but not the loop tubing). While the mechanism responsible for the different behavior is not understood, this potential variable will be considered further in future tests.

Unlike previous experiments, the loop tubing was not sectioned for destructive analysis following these tests. [Rather, the TCLs were preserved as close to undamaged as possible for reuse in scoping tests in another portion of this program.] However, at the openings of the tubing, no indications of wetting or other interaction of the Hg with the containment were noted.

4.0 CONCLUSIONS

Coupons of 316L stainless steel representing a wide variety of surface conditions and heat treatments were exposed to flowing Hg in a thermal convection loop for 2000 h. With the exception of gold-coated coupons, the coupon treatment and operation of the loop (pre-soak at 310°C prior to establishment of standard temperature gradient and temperatures) had only very minor influence on the compatibility of 316L with Hg. Similar to previously reported results,⁶ the areas of wetting/attack revealed a somewhat irregular and porous surface with substantial Ni and Cr depletion from this region. The gold-coated specimens revealed essentially complete wetting of the gold-coated side, which also developed significant surface roughness compared to the initial condition. Weight loss of the gold-coated coupons appears to occur at a significantly greater rate than for coupons wetted without the aid of gold, potentially related to the speed and completeness of the wetting reaction for the gold-coated surface. In any case, maximum penetration of any of the 316L coupons corresponds to about 15 μm in 2000 h at 300°C in Hg flowing at 1.2 m/s.

ACKNOWLEDGMENTS

The authors would like to acknowledge the helpful role of many individuals. H. F. Longmire performed the specimen metallography and E. A. Kenik performed the microprobe analysis. J. D. Hunn performed the iron implantations and H. M. Meyer and K. A. Thomas deposited the gold-coating. R. B. Ogle and S. N. Lewis provided Industrial Hygiene advice and services for controlling mercury exposures. J. H. DeVan provided many helpful discussions and insights, and P. F. Tortorelli provided critical review of the manuscript. F. C. Stooksbury and K. A. Choudhury helped prepare the manuscript and figures.

REFERENCES

1. L. K. Mansur and H. Ullmaier, compiled *Proceedings of the International Workshop on Spallation Materials Technology*, **CONF-9604151**, Oak Ridge, TN, April 23-25, 1996.
2. L. F. Epstein, in *Liquid Metals Technology – Part I*, F. J. Antwerpen, ed., “Static and Dynamic Corrosion and Mass Transfer in Liquid Metal Systems,” *Chemical Engineering Progress Symposium Series*, **53(20)**, p.67, 1957.
3. J. R. DiStefano, *A Review of the Compatibility of Containment Materials with Potential Liquid Metal Targets*, ORNL/TM-13056, August 1995.
4. J. R. Weeks, “Liquidus Curves and Corrosion of Fe, Cr, Ni, Co, V, Cb, Ta, Ti, and Zr in 500-750°C Mercury,” *Corrosion*, **23(4)**, p.98, 1967.
5. J. R. DiStefano, S. J. Pawel, and E. T. Mannes Schmidt, *Materials Compatibility Studies for the Spallation Neutron Source*, ORNL/TM-13675, September 1998.
6. S. J. Pawel, J. R. DiStefano, and E. T. Mannes Schmidt, *Corrosion of Type 316L Stainless Steel in a Mercury Thermal Convection Loop*, ORNL/TM-13754, April 1999.
7. S. J. Pawel, J. R. DiStefano, and E. T. Mannes Schmidt, *Corrosion of Alloy 718 in a Mercury Thermal Convection Loop*, ORNL/TM-1999/323, December 1999.
8. S. J. Pawel, “Literature Review on the Role of Nitrogen in Austenitic Steels,” *Steel Founders’ Research Journal*, **5**, p.1, 1984.
9. S. J. Pawel, E. E. Stansbury, and C. D. Lundin, “Role of Nitrogen in the Pitting Resistance of Cast Duplex CF-Type Stainless Steels,” *Corrosion*, **45(2)**, p.125, 1989.
10. K. Farrell and T. S. Byun, *Tensile Properties of Candidate SNS Target and Container Materials after Proton and Neutron Irradiation in the LANSCE Accelerator*, **SNS/TSR-193**, May 2000.
11. S. J. Pawel, et al., *Screening Test Results of Fatigue Properties of Type 316LN Stainless Steel in Mercury*, **ORNL/TM-13759**, March 1999.

INTERNAL DISTRIBUTION

- | | | | |
|-------|----------------------|--------|---|
| 1. | R. R. Allen | 28. | L. K. Mansur |
| 2. | R. E. Battle | 29. | T. E. Mason |
| 3. | E. E. Bloom | 30. | T. J. McManamy |
| 4. | K. K. Chipley | 31. | G. E. Michaels |
| 5. | J. E. Cleaves | 32. | D. E. Moncton |
| 6. | J. W. Cobb | 33. | A. E. Pasto |
| 7. | H. H. Cromwell | 34-38. | S. J. Pawel |
| 8. | J. H. DeVan | 39. | M. J. Rennich |
| 9-13. | J. R. DiStefano | 40. | S. L. Schrock |
| 14. | D. A. Everitt | 41. | P. T. Spampinato |
| 15. | K. Farrell | 42. | C. N. Strawbridge |
| 16. | T. A. Gabriel | 43. | J. P. Strizak |
| 17. | J. R. Haines | 44. | R. P. Taleyarkhan |
| 18. | L. L. Horton | 45. | P. T. Tortorelli |
| 19. | J. D. Hunn | 46. | J. H. Whealton |
| 20. | L. L. Jacobs | 47. | D. K. Wilfert |
| 21. | D. R. Johnson | 48. | G. T. Yahr |
| 22. | J. O. Johnson | 49. | G. L. Yoder |
| 23. | A. G. Jordan | 50-51. | Central Research Library |
| 24. | E. H. Lee | 52. | Document Reference Section |
| 25. | D. C. Lousteau | 53-54. | ORNL Laboratory Records-RC |
| 26. | A. T. Lucas | 55. | Office of Scientific & Technical
Information |
| 27. | E. T. Mannes Schmidt | | |

EXTERNAL DISTRIBUTION

56. G. Bauer, Paul Scherrer Institute, CH-5232, Villigen-PSI, Switzerland
57. J. M. Carpenter, Argonne National Laboratory, 9700 South Cass Avenue, Building 360, IPNS Division, Argonne, IL 60439
58. A. Jason, Los Alamos National Laboratory, P.O. Box 1663, H817 LANSCE-1, Los Alamos, NM 87545
59. P. Liaw, University of Tennessee, Department of Materials Science & Engineering, 427-B Dougherty Building, Knoxville, TN 37996-2200
60. W. Sommer, Los Alamos National Laboratory, P.O. Box 1663, LANSCE-2, Los Alamos, NM 87545
61. M. Todosow, Brookhaven National Laboratory, P.O. Box 5000, Building 475B, Upton, NY 11973
62. M. Wechsler, 106 Hunter Hill Place, Chapel Hill, NC 27514-9128
63. W. Weng, Brookhaven National Laboratory, P.O. Box 5000, Building 911B, Upton, NY 11973

